THE NUCLEAR SPIN SCISSORS MODE — THEORY AND EXPERIMENT*

E.B. Balbutsev, I.V. Molodtsova

Bogoliubov Laboratory of Theoretical Physics
Joint Institute for Nuclear Research
Dubna, 141980, Russia

P. Schuck

Institut de Physique Nucléaire, IN2P3-CNRS, Université Paris-Sud
91406 Orsay cédex, France
and
Laboratoire de Physique et Modélisation des Milieux Condensés, CNRS
and Université Joseph Fourier
25 avenue des Martyrs BP166, 38042 Grenoble cédex 9, France

(Received December 21, 2018)

The fine structure of the scissors mode is investigated within the Wigner Function Moments (WFM) method. The solution of time-dependent Hartree–Fock–Bogoliubov equations by WFM method with the isovector–isoscalar coupling taken into account predicts splitting of the scissors mode into three branches. Together with the conventional scissors mode generated by the counter-rotation of protons against neutrons, two new modes arise when the spin degrees of freedom are taken into account. First, we turn to ^{160,162,164}Dy isotopes. Accounting for spin scissors allows to explain the nature of two groups of M1 excitations with an anomalously large summed magnetic strength experimentally detected in ^{164}Dy. A comparison with the recently reanalyzed data of Oslo-type experiments is presented.

DOI:10.5506/APhysPolBSupp.12.637

1. Introduction

In Ref. [1], the Wigner Function Moments (WFM) or phase-space moments method was applied for the first time to solve the time-dependent Hartree–Fock–Bogoliubov (TDHFB) equations including spin dynamics. As

* Presented at the XXV Nuclear Physics Workshop "Structure and Dynamics of Atomic Nuclei", Kazimierz Dolny, Poland, September 25–30, 2018.

a first step, only the spin–orbit interaction was included in the consideration, as the most important one among all possible spin-dependent interactions because it enters into the mean field. The most remarkable result was the prediction of a new type of nuclear collective motion: rotational oscillations of "spin-up" nucleons with respect of "spin-down" nucleons (the spin scissors mode). This new type of nuclear scissors complements the conventional (orbital) scissors mode. Later, its undoubted traces were found in actinides and in rare-earth nuclei [2].

By definition, the scissors mode is the pure isovector mode. That is why we divided the dynamical equations describing collective motion (including scissors) into isovector and isoscalar parts with the aim to separate the pure scissors mode. It is impossible to perform such separation exactly in the realistic case, so one is forced to use some approximate procedure. In this way, we achieved the satisfactory agreement with experimental data [2]. To test the used approximation, we now solved the coupled dynamical equations for protons and neutrons exactly, without the artifical isovector–isoscalar decoupling. As a result, one more magnetic mode (third type of scissors) appeared. Actually, the existence of three scissors states is easily explained by combinatoric consideration — there are only three ways to divide the four different kinds of objects (spin-up and spin-down protons and neutrons in our case) into two pairs. The analysis of the new situation which appeared due to the last findings in the description of nuclear scissors is presented in this paper.

2. Isovector–isoscalar coupling

Let us consider the simple model of the harmonic oscillator with q–q residual interaction

$$H = \sum_{i=1}^{A}\left(\frac{\boldsymbol{p}_i^2}{2m}+\frac{1}{2}m\omega^2\boldsymbol{r}_i^2\right) + \sum_{\mu=-2}^{2}(-1)^{\mu}\left\{\bar{\kappa}\sum_{i}^{Z}\sum_{j}^{N}+\frac{\kappa}{2}\left[\sum_{i\neq j}^{Z}+\sum_{i\neq j}^{N}\right]\right\}q_{2\mu}(\boldsymbol{r}_i)q_{2-\mu}(\boldsymbol{r}_j)\,, \qquad (1)$$

where $q_{2\mu}=\sqrt{16\pi/5}\,r^2Y_{2\mu}$ and N, Z are the number of neutrons and protons, respectively.

Integrating the equation for the Wigner function $f^{\tau}(\boldsymbol{r},\boldsymbol{p},t)$ over phase space with the weights $\{r\otimes r\}_{\lambda\mu}$, $\{p\otimes p\}_{\lambda\mu}$, $\{r\otimes p\}_{\lambda\mu}$, one gets dynamical equations for the following second order moments-collective variables:

$$
\begin{aligned}
R^{\tau}_{\lambda\mu}(t) &= 2(2\pi\hbar)^{-3}\int \mathrm{d}\boldsymbol{p}\int \mathrm{d}\boldsymbol{r}\,\{r\otimes r\}_{\lambda\mu} f^{\tau}(\boldsymbol{r},\boldsymbol{p},t)\,,\\
P^{\tau}_{\lambda\mu}(t) &= 2(2\pi\hbar)^{-3}\int \mathrm{d}\boldsymbol{p}\int \mathrm{d}\boldsymbol{r}\,\{p\otimes p\}_{\lambda\mu} f^{\tau}(\boldsymbol{r},\boldsymbol{p},t)\,,\\
L^{\tau}_{\lambda\mu}(t) &= 2(2\pi\hbar)^{-3}\int \mathrm{d}\boldsymbol{p}\int \mathrm{d}\boldsymbol{r}\,\{r\otimes p\}_{\lambda\mu} f^{\tau}(\boldsymbol{r},\boldsymbol{p},t)\,. \qquad (2)
\end{aligned}
$$

Isoscalar and isovector variables are defined as $X_{\lambda\mu}(t) = X^{n}_{\lambda\mu}(t) + X^{p}_{\lambda\mu}(t)$, $\bar{X}_{\lambda\mu}(t) = X^{n}_{\lambda\mu}(t) - X^{p}_{\lambda\mu}(t)$, where $X \equiv \{R, L, P\}$. Coupled nonlinear isovector and isoscalar dynamical equations read

$$
\begin{aligned}
\dot{\bar{R}}_{\lambda\mu} &= \frac{2}{m}\bar{L}_{\lambda\mu}\,,\\
\dot{\bar{L}}_{\lambda\mu} &= \frac{1}{m}\bar{P}_{\lambda\mu} - m\,\omega^2\bar{R}_{\lambda\mu} + 12\sqrt{5}\sum_{j=0}^{2}\sqrt{2j+1}\begin{Bmatrix}11j\\2\lambda 1\end{Bmatrix}\\
&\quad\times\left[\kappa_0\left\{R_2\otimes\bar{R}_j\right\}_{\lambda\mu} + \kappa_1\left\{\bar{R}_2\otimes R_j\right\}_{\lambda\mu}\right]\,,\\
\dot{\bar{P}}_{\lambda\mu} &= -2m\,\omega^2\bar{L}_{\lambda\mu} + 24\sqrt{5}\sum_{j=0}^{2}\sqrt{2j+1}\begin{Bmatrix}11j\\2\lambda 1\end{Bmatrix}\\
&\quad\times\left[\kappa_0\left\{R_2\otimes\bar{L}_j\right\}_{\lambda\mu} + \kappa_1\left\{\bar{R}_2\otimes L_j\right\}_{\lambda\mu}\right]\,,\\
\dot{R}_{\lambda\mu} &= \frac{2}{m}L_{\lambda\mu}\,,\\
\dot{L}_{\lambda\mu} &= \frac{1}{m}P_{\lambda\mu} - m\,\omega^2 R_{\lambda\mu} + 12\sqrt{5}\sum_{j=0}^{2}\sqrt{2j+1}\begin{Bmatrix}11j\\2\lambda 1\end{Bmatrix}\\
&\quad\times\left[\kappa_0\{R_2\otimes R_j\}_{\lambda\mu} + \kappa_1\left\{\bar{R}_2\otimes\bar{R}_j\right\}_{\lambda\mu}\right]\,,\\
\dot{P}_{\lambda\mu} &= -2m\,\omega^2 L_{\lambda\mu} + 24\sqrt{5}\sum_{j=0}^{2}\sqrt{2j+1}\begin{Bmatrix}11j\\2\lambda 1\end{Bmatrix}\\
&\quad\times\left[\kappa_0\{R_2\otimes L_j\}_{\lambda\mu} + \kappa_1\left\{\bar{R}_2\otimes\bar{L}_j\right\}_{\lambda\mu}\right]\,, \qquad (3)
\end{aligned}
$$

where $\kappa_0 = (\kappa + \bar{\kappa})/2$, $\kappa_1 = (\kappa - \bar{\kappa})/2$ — strength constants connected by the relation $\kappa_1 = \alpha\kappa_0$ [1]. Equations (3) are solved in a small amplitude approximation. To this end, all collective variables are written as $X_{\lambda\mu}(t) = X^{\mathrm{eq}}_{\lambda\mu} + \mathcal{X}_{\lambda\mu}(t)$, where $\mathcal{X}_{\lambda\mu}(t)$ is an infinitesimally small deviation, and equations (3) are linearized by neglecting $\mathcal{X}_{\lambda\mu}(t)^2$ terms

$$\dot{\bar{\mathcal{R}}}_{\lambda\mu} = \frac{2}{m}\bar{\mathcal{L}}_{\lambda\mu}\,, \tag{4}$$

$$\begin{aligned}\dot{\bar{\mathcal{L}}}_{\lambda\mu} &= \frac{1}{m}\bar{\mathcal{P}}_{\lambda\mu} - m\,\omega^2\bar{\mathcal{R}}_{\lambda\mu} + 12\sqrt{5}\sum_{j=0}^{2}\sqrt{2j+1}\begin{Bmatrix}11j\\2\lambda 1\end{Bmatrix}\\ &\times\Bigg[\kappa_0\left\{R_2^{\rm eq}\otimes\bar{\mathcal{R}}_j\right\}_{\lambda\mu} + \kappa_1\left\{\bar{\mathcal{R}}_2\otimes R_j^{\rm eq}\right\}_{\lambda\mu}\\ &+ \underbrace{\kappa_1\left\{\bar{R}_2^{\rm eq}\otimes\mathcal{R}_j\right\}_{\lambda\mu} + \kappa_0\left\{\mathcal{R}_2\otimes\bar{R}_j^{\rm eq}\right\}_{\lambda\mu}}_{\textbf{coupling terms}}\Bigg]\,,\end{aligned} \tag{5}$$

$$\begin{aligned}\dot{\bar{\mathcal{P}}}_{\lambda\mu} &= -2m\,\omega^2\bar{\mathcal{L}}_{\lambda\mu} + 24\sqrt{5}\sum_{j=0}^{2}\sqrt{2j+1}\begin{Bmatrix}11j\\2\lambda 1\end{Bmatrix}\\ &\times\Bigg[\kappa_0\left\{R_2^{\rm eq}\otimes\bar{\mathcal{L}}_j\right\}_{\lambda\mu} + \kappa_1\left\{\bar{\mathcal{R}}_2\otimes L_j^{\rm eq}\right\}_{\lambda\mu}\\ &+ \underbrace{\kappa_1\left\{\bar{R}_2^{\rm eq}\otimes\mathcal{L}_j\right\}_{\lambda\mu} + \kappa_0\left\{\mathcal{R}_2\otimes\bar{L}_j^{\rm eq}\right\}_{\lambda\mu}}_{\textbf{coupling terms}}\Bigg]\,,\end{aligned} \tag{6}$$

$$\dot{\mathcal{R}}_{\lambda\mu} = \frac{2}{m}\mathcal{L}_{\lambda\mu}\,, \tag{7}$$

$$\begin{aligned}\dot{\mathcal{L}}_{\lambda\mu} &= \frac{1}{m}\mathcal{P}_{\lambda\mu} - m\,\omega^2\mathcal{R}_{\lambda\mu} + 12\sqrt{5}\sum_{j=0}^{2}\sqrt{2j+1}\begin{Bmatrix}11j\\2\lambda 1\end{Bmatrix}\\ &\times\Bigg[\kappa_0\left(\left\{R_2^{\rm eq}\otimes\mathcal{R}_j\right\}_{\lambda\mu} + \left\{\mathcal{R}_2\otimes R_j^{\rm eq}\right\}_{\lambda\mu}\right)\\ &+ \underbrace{\kappa_1\left(\left\{\bar{R}_2^{\rm eq}\otimes\bar{\mathcal{R}}_j\right\}_{\lambda\mu} + \left\{\bar{\mathcal{R}}_2\otimes\bar{R}_j^{\rm eq}\right\}_{\lambda\mu}\right)}_{\textbf{coupling terms}}\Bigg]\,,\end{aligned} \tag{8}$$

$$\begin{aligned}\dot{\mathcal{P}}_{\lambda\mu} &= -2m\,\omega^2\mathcal{L}_{\lambda\mu} + 24\sqrt{5}\sum_{j=0}^{2}\sqrt{2j+1}\begin{Bmatrix}11j\\2\lambda 1\end{Bmatrix}\\ &\times\Bigg[\kappa_0\left(\left\{R_2^{\rm eq}\otimes\mathcal{L}_j\right\}_{\lambda\mu} + \left\{\mathcal{R}_2\otimes L_j^{\rm eq}\right\}_{\lambda\mu}\right)\end{aligned}$$

$$+ \underbrace{\kappa_1 \left(\left\{ \bar{R}_2^{\mathrm{eq}} \otimes \bar{\mathcal{L}}_j \right\}_{\lambda\mu} + \left\{ \bar{\mathcal{R}}_2 \otimes \bar{L}_j^{\mathrm{eq}} \right\}_{\lambda\mu} \right)}_{\text{coupling terms}} \Bigg] . \tag{9}$$

Let us analyse, for example, the structure of the coupling terms in the isovector equation (5): $\kappa_1\{\bar{R}_2^{\mathrm{eq}} \otimes \mathcal{R}_j\}_{\lambda\mu} + \kappa_0\{\mathcal{R}_2 \otimes \bar{R}_j^{\mathrm{eq}}\}_{\lambda\mu}$. The isoscalar variables $\mathcal{R}$ are coupled through the difference of the equilibrium characteristics of the proton and neutron systems $\bar{R}^{\mathrm{eq}}$. There are two methods to decouple the equations:

1. Just neglect by the coupling terms, that is equivalent to the assumption that all equilibrium characteristics of protons are equal to that of neutrons.

2. One assumes that all amplitudes (deviations) of protons are proportional to that of neutrons: $\mathcal{X}_{\lambda\mu}^{p}/Z = \pm\mathcal{X}_{\lambda\mu}^{n}/N$ (+ for isoscalar motion, − for isovector one).

Both methods produce similar results. In our previous papers [1–4], we used the first method. Taking into account the pair correlations and spin degrees of freedom, we obtained the set of 22 coupled isovector equations and the same number of isoscalar equations. Excluding the integrals of motion, we obtained 14 non-zero solutions.

3. Effect of the coupling terms

The results of our calculations are presented in Table I, where the energies, magnetic dipole and electric quadrupole strength are shown for ^{164}Dy. Left panel — the solutions of decoupled equations, right — isovector–isoscalar coupling terms are taken into account. Solutions of the isovector system of decoupled equations are marked as IV and isoscalar solutions are marked as IS. The first observation is that the high-lying levels are less sensitive to decoupling. Among the high-lying states, $\mu = 1$ branches of isoscalar (at the energy of 10.94 MeV) and isovector ($E_i = 21.29$ MeV) Giant Quadrupole Resonances are distinguished by a large B(E2) values. The rest of high-lying states have quite small excitation probabilities and we omit them in further discussion. The lowest electric level has a complicated origin and we have not considered it so far.

Comparing the left and right panels, we see that the most remarkable change happens with the third low-lying level — it acquires rather big magnetic strength. So, in the decoupled case, there are 2 isoscalar electric and 2 isovector magnetic low-lying levels, and in the coupled case, there are 1 electric and 3 magnetic levels of mixed isovector–isoscalar nature. These

TABLE I

The results of WFM calculations for ^{164}Dy: energies E_i, magnetic dipole $B(\mathrm{M1})_i$ and electric quadrupole $B(\mathrm{E2})_i$ strength. IS — isoscalar, IV — isovector.

	Decoupled equations			Coupled equations		
	E_i [MeV]	$B(\mathrm{M1})_i$ $[\mu_N^2]$	$B(\mathrm{E2})_i$ [W.u.]	E_i [MeV]	$B(\mathrm{M1})_i$ $[\mu_N^2]$	$B(\mathrm{E2})_i$ [W.u.]
IS	1.29	0.01	53.25	1.47	0.17	25.44
IV	**2.44**	**2.03**	0.34	**2.20**	**1.76**	3.30
IS	**2.62**	**0.09**	2.91	**2.87**	**2.24**	0.34
IV	**3.35**	**1.36**	1.62	**3.59**	**1.56**	4.37
IS	10.94	0.00	55.12	10.92	0.04	50.37
IV	14.04	0.00	2.78	13.10	0.00	2.85
IS	14.60	0.06	0.48	15.42	0.07	0.57
IV	15.88	0.00	0.55	15.55	0.00	1.12
IS	16.46	0.07	0.36	16.78	0.06	0.53
IV	17.69	0.00	0.45	17.69	0.01	0.68
IS	17.90	0.00	0.51	17.91	0.00	0.53
IV	18.22	0.18	1.85	18.22	0.13	0.89
IS	19.32	0.10	0.97	19.32	0.08	0.61
IV	21.29	2.47	31.38	21.26	2.03	21.60

three magnetic states correspond to three physically possible scissors modes. They are all generated by oscillations of the orbital angular momenta. The state at the energy of 3.59 MeV is the conventional "orbital" scissors mode, the last two states at the energies of 2.20 MeV and 2.87 MeV are the "spin" scissors modes. The difference between "orbital" and "spin" scissors is that the "orbital" scissors are generated by the counter-oscillations of the orbital angular momentum of proton body with respect to the orbital angular momentum of neutron body, whereas the "spin" scissors are generated by the counter-oscillations of the orbital angular momentum of nucleons with spin projection "up" with respect to the orbital angular momentum of nucleons with spin projection "down".

Figure 1 shows a schematic representation of these modes: the orbital scissors (neutrons *versus* protons) and two spin scissors (spin-up nucleons *versus* spin-down nucleons and more complicated — spin-up protons together with spin-down neutrons *versus* spin-down protons jointed with spin-up neutrons). Both spin scissors exist only due to the spin degrees of freedom. If we remove the arrows from the picture, nothing will change for the conventional scissors (a). However, figures (b) and (c) in this case become identical, the division of neutrons and protons in two parts being pointless.

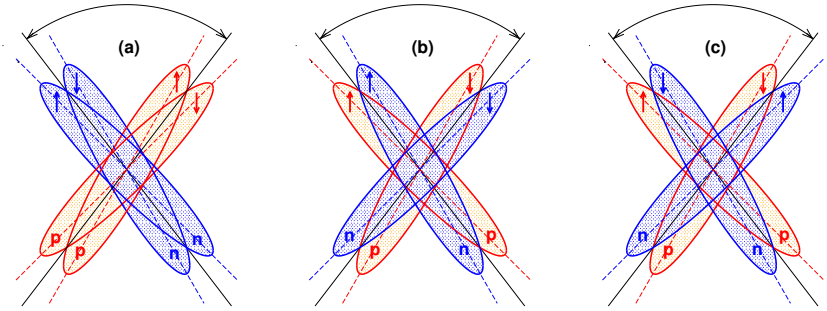

Fig. 1. (Colour on-line) Schematic representation of three interconnected scissors modes: (a) spin-scalar isovector (conventional, orbital scissors), (b) spin-vector isoscalar (spin scissors) and (c) spin-vector isovector (spin scissors). Arrows show the direction of spin projections; p — protons, n — neutrons. Grey/blue and light grey/orange ellipses are slightly tilted only for presentation reasons: in reality, they fully overlap.

The isovector–isoscalar coupling strongly mixes the two spin-vector states. Strictly speaking, interpretation in terms of isovector–isoscalar excitations loses its significance, especially for spin scissors. Rather, it is more correct to speak about the associated response of protons and neutrons. Only the classification in terms of spin-scalar and spin-vector remains valid. As follows from our calculations, the spin scissors are lower in energy and stronger in transition probability than the orbital scissors.

When we try to compare the theoretical results with the existing experimental data for the scissors mode, we encounter different summing interval conventions. It is assumed that scissors mode includes only the states in a certain energy range. As a rule, the following two conventions are chosen, which leads to slightly different results for the summed M1 strength: $2.7 < E < 3.7$ MeV for $Z < 68$ and $2.4 < E < 3.7$ MeV for $Z \geq 68$ [5], $2.5 < E < 4.0$ MeV for $82 \leq N \leq 126$ [6]. Figure 2 demonstrates the excitation energy spectra of ^{160,162,164}Dy isotopes with the corresponding B(M1) values obtained by the Nuclear Resonance Fluorescence (NRF) experiment [7]. The dash lines mark the boundaries of the conventional interval [5]. Obviously, there are two groups of strong M1 excitations in ^{164}Dy around 2.6 and 3.1 MeV. Usually, only the upper group is attributed to the scissors mode, and the group of around 2.6 MeV is not included. The strongest argument to exclude the lower group of M1 excitations from the scissors mode systematics is the significant spin contribution into the magnetic strength of this group.

Taking into account isovector–isoscalar coupling allows one to explain the nature of two groups of 1^+ levels with an anomalously large summed magnetic strength in ^{164}Dy. Table II demonstrates that the energy centroid

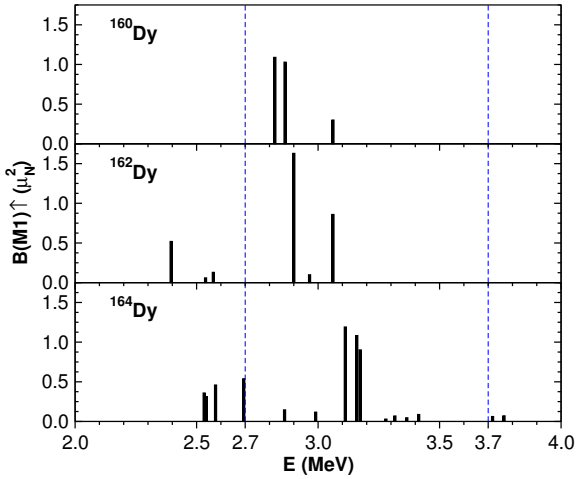

Fig. 2. Excitation energies E with the corresponding $B(\mathrm{M1})$ values, obtained by the NRF experiment [7]. The dashed lines mark the boundaries of the conventional interval from [5].

and summed (total, including the spin contribution) $B(\mathrm{M1})$-value of the lower group of the experimental 1^+ states agree very well with the calculated E and $B(\mathrm{M1})$ of the lowest spin-vector level. The respective values of the higher group are in excellent agreement with the energy centroid and summed $B(\mathrm{M1})$ of the remaining spin-vector and spin-scalar states.

Summation over all excitation energies (presented in the last line of the table) also gives very good agreement with the theory. According to our calculations, the lower-energy group of states (which is usually neglected by experimentalists) also represents a scissors mode (spin scissors).

TABLE II

The energies E_i with excitation probabilities $B(\mathrm{M1})_i$ of three scissors and energy centroids $\bar{E}$ and summed $\sum B(\mathrm{M1})$ of the spin-vector and spin-scalar states are compared with experimental values $\bar{E}$ and $\sum B(\mathrm{M1})$ of two groups of 1^+ levels in ^{164}Dy [7]. The results of summation over all excitation energies are shown in the last line.

	Theory (WFM)			Experiment	
E_i [MeV]	$B(\mathrm{M1})_i$ [μ_N^2]	$\bar{E}$ [MeV]	$\sum B(\mathrm{M1})$ [μ_N^2]	$\bar{E}$ [MeV]	$\sum B(\mathrm{M1})$ [μ_N^2]
2.20	1.76	2.20	1.76	2.60	1.67(14)
2.87	2.24	3.17	3.80	3.17	3.85(31)
3.59	1.56				
		2.86	5.56	3.00	5.52(48)

The calculations have shown that the scissors mode is not pure isovector. All three scissors modes have an underlying orbital nature, because all are generated by the same type of collective variables — the orbital angular momenta. At the same time, they are strongly sensitive to the influence of the spin-dependent part of the external field. It is demonstrated in Table III, where the results of calculations of $B(\mathrm{M1})$ with ($g_\mathrm{s} = 0.7 g_\mathrm{s}^\mathrm{free}$) and without ($g_\mathrm{s} = 0$) the spin part of a dipole magnetic operator are presented. Comparison of the second and third columns of the table allows one to observe a moderate constructive interference of the orbital and spin contributions in the case of the spin scissors modes and their very strong destructive interference in the case of the orbital scissors mode.

TABLE III

The results of WFM calculations of $B(\mathrm{M1})$ with ($g_\mathrm{s} = 0.7 g_\mathrm{s}^\mathrm{free}$) and without ($g_\mathrm{s} = 0$) the spin part of a dipole magnetic operator are shown for three scissors modes with energies E_i.

E_i [MeV]	$B(\mathrm{M1})_i$ [μ_N^2]	
	$g_\mathrm{s} = 0.7 g_\mathrm{s}^\mathrm{free}$	$g_\mathrm{s} = 0$
2.20	1.76	0.53
2.87	2.24	1.52
3.59	1.56	6.63

In a recent paper [8], the authors revised their previous data on the $^{160-164}$Dy obtained in the framework of the Oslo method. It was concluded that the presented results and previous investigations [9] experimentally confirm the validity of the generalized Brink hypothesis for the scissors resonance (SR). The summed strengths of SR were compared with NRF [7] and (n, γ) measurements [10]. The same strength was found provided that the integration limits for the summed SR strength were used, similar to those used for the NRF experiments. A quotation from the above paper [8]: "... If we integrate over all transition energies, we find a total, summed SR strength of 4–5 μ^2. The present fit strategy gives about 40% higher summed SR strengths than the reported NRF results. However, if we apply the NRF energy limits, we obtain excellent agreement with the NRF results. It is interesting to note that $\sim$ 40–60% of our measured SR strength lies in the energy region below 2.7 MeV. In traditional NRF experiments using bremsstrahlung, the transitions in this energy range are quite difficult to separate from the sizable atomic background."

Let us compare our latest results with the above experimental findings of the Oslo group. The comparison of the energy centroids and corresponding summed SR strength from the WFM theory with the Quasiparticle-Phonon Nuclear Model (QPNM) calculations [11, 12], experimental results from the NRF, and, in addition, from photo-neutron measurements (Oslo) is presented in Table IV and Fig. 3. Comparison is presented for energy interval from 2.7 to 3.7 MeV and for the appropriate extended energy regions. As it is seen from Table IV, the theoretical results and experimental data are in very good overall agreement. The experimental results obtained by the radiative capture of resonance neutrons [10] are also added in Fig. 3.

TABLE IV

The energy centroids $\bar{E}$ and corresponding summed SR strength $B(\mathrm{M1})$ from the WFM theory are compared with the QPNM calculations [11, 12], experimental results by the NRF [7] and photo-neutron measurements (Oslo) [8] for ^{160,162,164}Dy. Comparison is presented for two energy intervals.

^{A}Dy	Theory			Experiment			
	WFM		QPNM	NRF		Oslo	
	$\bar{E}$ [MeV]	$B(\mathrm{M1})$ [μ_N^2]	$B(\mathrm{M1})$ [μ_N^2]	$\bar{E}$ [MeV]	$B(\mathrm{M1})$ [μ_N^2]	$\bar{E}$ [MeV]	$B(\mathrm{M1})$ [μ_N^2]
^{160}Dy	$2.7 < E < 3.7$ MeV						
	3.17	3.35	2.46	2.87	2.42(30)	2.66(12)	1.7(10)
	$2.0 < E < 3.7$ MeV			$2.5 < E < 4.0$ MeV		$0 < E < 10$ MeV	
	2.84	5.19	4.61	2.87	2.42(30)	2.66(12)	4.8(26)
^{162}Dy	$2.7 < E < 3.7$ MeV						
	3.16	3.58	2.60	2.96	2.59(19)	2.81(8)	2.3(8)
	$2.0 < E < 3.7$ MeV			$2.5 < E < 4.0$ MeV		$0 < E < 10$ MeV	
	2.85	5.38	4.68	2.84	3.30(24)	2.81(8)	4.8(17)
^{164}Dy	$2.7 < E < 3.7$ MeV						
	3.17	3.80	2.92	3.17	3.85(31)	2.83(8)	2.8(9)
	$2.0 < E < 3.9$ MeV			$2.5 < E < 4.0$ MeV		$0 < E < 10$ MeV	
	2.86	5.56	5.10	3.00	5.52(48)	2.83(8)	5.5(18)

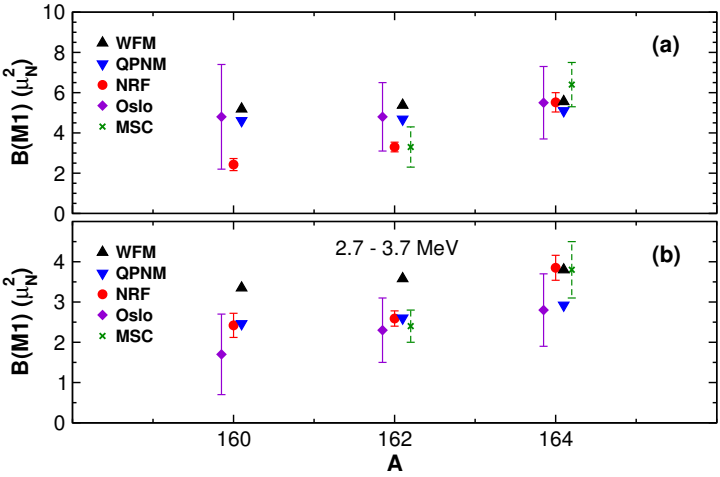

Fig. 3. Summed SR strength B(M1) from the QPNM calculations [11, 12], experimental results obtained by the NRF [7], photo-neutron measurements (Oslo) [8] and radiative capture of resonance neutrons [10] are compared with WFM results. (a) the results of summation over the extended energy regions, (b) for energy interval from 2.7 to 3.7 MeV.

4. Conclusion

The dynamical equations describing the nuclear collective motion are solved exactly, without the artificial division into isovector and isoscalar parts. As a result, a new type (third one) of nuclear scissors is found. Three types of scissors can be classified as isovector spin-scalar (conventional), isovector spin-vector and isoscalar spin-vector. The isovector–isoscalar coupling strongly mixes the two spin-vector states. The calculated energy centroids and summarized transition probabilities of Dy isotopes are in very good agreement with the experimental results of the Oslo group. The experimental NRF data for ^{164}Dy are in excellent agreement with our calculations, whereas the data for ^{160,162}Dy are in good agreement only with calculated centroids of two higher lying scissors: isovector spin-scalar one + isoscalar spin-vector one. Thus, we agree with the conclusion of the authors of [8]: "It is highly desirable to remeasure the Dy isotopes by performing NRF experiments using quasi-monochromatic beams in the interesting energy region between 2 and 4 MeV as done for ^{232}Th."

REFERENCES

[1] E.B. Balbutsev, I.V. Molodtsova, P. Schuck, *Nucl. Phys. A* **872**, 42 (2011).

[2] E.B. Balbutsev, I.V. Molodtsova, P. Schuck, *Phys. Rev. C* **97**, 044316 (2018).

[3] E.B. Balbutsev, I.V. Molodtsova, P. Schuck, *Phys. Rev. C* **88**, 014306 (2013).

[4] E.B. Balbutsev, I.V. Molodtsova, P. Schuck, *Phys. Rev. C* **91**, 064312 (2015).

[5] N. Pietralla *et al.*, *Phys. Rev. C* **52**, R2317 (1995).

[6] J. Enders *et al.*, *Phys. Rev. C* **71**, 014306 (2005).

[7] J. Margraf *et al.*, *Phys. Rev. C* **52**, 2429 (1995).

[8] T. Renstrøm *et al.*, *Phys. Rev. C* **98**, 054310 (2018) [arXiv:1804.07654 [nucl-ex]].

[9] M. Guttormsen *et al.*, *Phys. Rev. Lett.* **116**, 012502 (2016).

[10] S. Valenta *et al.*, *Phys. Rev. C* **96**, 054315 (2017).

[11] V.G. Soloviev, A.V. Sushkov, N.Yu. Shirikova, *Phys. Part. Nucl.* **31**, 385 (2000).

[12] V.G. Soloviev *et al.*, *Nucl. Phys. A* **600**, 155 (1996).